Detecting the Universal Fractional Entropy of Majorana Zero Modes

Eran Sela,[1,2,3] Yuval Oreg,[4] Stephan Plugge,[2,3] Nikolaus Hartman,[2,3,†] Silvia Lüscher,[2,3] and Joshua Folk[2,3,*]
[1]Raymond and Beverly Sackler School of Physics and Astronomy, Tel-Aviv University, IL-69978 Tel Aviv, Israel
[2]Stewart Blusson Quantum Matter Institute, University of British Columbia, Vancouver, British Columbia V6T1Z4, Canada
[3]Department of Physics and Astronomy, University of British Columbia, Vancouver, British Columbia V6T1Z1, Canada
[4]Department of Condensed Matter Physics, Weizmann Institute of Science, Rehovot 76100, Israel

(Received 7 June 2019; published 2 October 2019)

A pair of Majorana zero modes (MZMs) constitutes a nonlocal qubit whose entropy is log2. Upon strongly coupling one of the constituent MZMs to a reservoir with a continuous density of states, a universal entropy change of $\frac{1}{2}\log 2$ is expected to be observed across an intermediate temperature plateau. We adapt the entropy-measurement scheme that was the basis of a recent experiment by Hartman *et al.* [Nat. Phys. **14**, 1083 (2018)] to the case of a proximitized topological system hosting MZMs and propose a method to measure this $\frac{1}{2}\log 2$ entropy change—an unambiguous signature of the nonlocal nature of the topological state. This approach offers an experimental strategy to distinguish MZMs from non topological states.

DOI: 10.1103/PhysRevLett.123.147702

Introduction.—The Majorana qubit is a nonlocal two-level system formed by two Majorana zero modes (MZMs). These MZMs may appear, for example, in vortices of topological superconductors [1–3], as quasiparticles of exotic fractional quantum Hall states [1], or at the edges of (quasi) 1D topological superconductors [4–14]. Despite an enormous body of theoretical and experimental work [7,15,16], there is not yet conclusive evidence of the nonlocal nature of these zero modes that would distinguish them from non topological states. In this Letter, we propose an alternative direction towards this goal based on entropy measurements.

Traditional techniques for measuring entropy are difficult to apply to MZMs, due to the relatively large background contribution of the phonon bath in materials or devices that would host them. Recent progress has been achieved towards measuring the entropy of fractional quantum Hall quasiparticles via thermalization times [17] or thermoelectric effects [18–20] and using thermopower to extract entropy changes in quantum dot states [21]. Another efficient way to measure entropy in electronic nanostructures is via the temperature dependence of charge transitions, relying on a Maxwell thermodynamic relation $(dS/d\mu)|_T = (dN/dT)|_\mu$ that connects changes in the entropy S with chemical potential μ to changes in the particle number N with temperature T [22–24]. This idea was implemented in an experiment measuring the log2 entropy of a spinful quantum dot (QD) in the Coulomb blockade regime using a charge detector [25].

Here, we show theoretically that the approach in Ref. [25] can be applied to measure the nontrivial entropy associated with MZMs at the ends of 1D topological superconductors. Our discussion focuses mainly on semiconducting nanowires [4–10], but the approach is general and should apply to any system hosting MZMs—even fully open systems like quasi-one-dimensional Josephson junctions [11–14]. Two factors make the measurement of MZM entropy more challenging than that of spin. First, MZMs naturally come in pairs, as in the Majorana qubit, which like any two-level system has the trivial entropy log2. Accessing the topological character of the MZM requires a measurement protocol that can resolve the entropy of an individual MZM. We build on the problem of impurity entropy in the two-channel Kondo model [26,27], which maps to a MZM coupled to a lead with a continuous density of states [28,29]. In this case, a universal $\frac{1}{2}\log 2$ entropy plateau [30] can be observed that provides the tell-tale signature of the nonlocal MZM state.

Second, this measurement protocol is sensitive only to *changes* in entropy, not to the absolute entropy of a state. In a spinful QD, one can start from the case of zero electrons ($N = 0$, hence $S = 0$) and then, using a gate voltage to add electrons, build up the entropy of higher charge states one by one. But MZM entropy is not directly dependent on N, that is, on the parity of the MZM-hosting island. We develop a scheme in which the topological $\frac{1}{2}\log 2$ entropy of a Majorana qubit coupled to a single lead can be turned on or off by the charge on a sensor QD. The total entropy of dot plus qubit is then N dependent, providing access to the MZM state via the protocol in Ref. [25].

The measurement we propose is laid out in Fig. 1: a quantum circuit that contains a Majorana qubit (we consider a wire with MZMs, γ_1 and γ_2, at either end), with γ_1 coupled to a lead across a barrier whose height depends electrostatically on the charge (eN) of a nearby QD. The QD is in the Coulomb blockade regime with energy $E(N) = E_c N^2 - \mu N$, where E_c is the charging energy. N

is controlled by the chemical potential μ of a reservoir from which electrons can tunnel onto the dot, although in an experiment μ would presumably be fixed and N would be tuned by an electrostatic gate. Charge steps $N \to N+1$ are measured by a nearby charge detector.

The rest of the Letter describes how this circuit can measure the $\frac{1}{2}\log 2$ entropy of a single MZM. Crucially, we find that the entropic signature of a MZM is a robust $\frac{1}{2}\log 2$, while that of an Andreev bound state (ABS) accidentally tuned to zero energy may be anywhere between the trivial log2 and $\frac{1}{2}\log 2$. Low-energy ABSs are often feared to mimic MZMs in conductance measurements. A strategy to distinguish the two scenarios by their entropy offers an important step forward.

Entropy detection method.—Consider a system whose free energy $F = F(N)$ depends on the charge N of a QD external to the system. In Fig. 1, the system is delineated by the dashed box and F depends on N via the coupling $V(N)$ between γ_1 and the lead. Within this framework, changes in the system entropy are reflected by the temperature dependence of charge steps in the QD. While the QD affects the system electrostatically, at finite T there is a thermodynamic backaction of the system on the QD, giving higher weight to charge states with higher entropy.

The charge on the dot is a minimization of a thermodynamic potential that is affected both by the QD and by the system. With a reservoir at chemical potential μ, the total partition function of the system and QD at temperature T is

$$Z_{\rm tot}(\mu, T) = \sum_N e^{-\{[F(N)+E(N)]/T\}}. \tag{1}$$

The QD is assumed to be spinless, although including QD spin would not change our results significantly. The average number of electrons on the QD is $N(\mu) = T(d\log Z_{\rm tot}/d\mu)$, and the total entropy of the combined QD and system is $S_{\rm tot} = -dF_{\rm tot}/dT$, where $F_{\rm tot} = -T\log Z_{\rm tot}$. The system's entropy can be readily separated from the total by subtracting the trivial entropy of the QD, which is log2 at the charge degeneracy points and drops exponentially to zero away from these points.

Figure 1 shows an example of QD charge steps $N(\mu)$, induced by raising the reservoir chemical potential. The charge steps broaden with T and also shift to the left, an effect that can be understood by integrating the Maxwell relation $(dS_{\rm tot}/d\mu)|_T = (dN/dT)|_\mu$,

$$\Delta S_{\rm tot}|_{\mu_1\to\mu_2} = \frac{d}{dT}\int_{\mu_1}^{\mu_2} N(\mu)d\mu. \tag{2}$$

Graphically, the entropy change $\Delta S_{\rm tot}$ is given by the temperature-induced variation of the area beneath the curve $N(\mu)$. The horizontal leftward shift of each step with increasing temperature indicates that the system entropy is increasing with N.

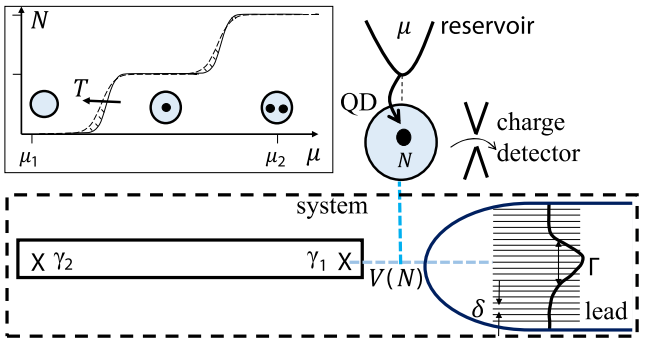

FIG. 1. Schematics of the proposed entropy measurement. The "system" consists of a Majorana qubit with two MZMs, with γ_1 coupled to a lead via coupling V that is sensitive to the charge N on a nearby QD in the Coulomb blockade regime. QD charge steps, from N to $N+1$, can be detected by a nearby sensor and induced by raising the chemical potential μ on a reservoir tunnel coupled to the QD. In the graph, the leftward shift of the charge steps with increasing temperature indicates entropy changes [Eq. (2)].

Before proceeding with the analysis of MZM entropy detection, it is helpful to compare the experimental protocol proposed here with the measurement described in Ref. [25]. In that case, the measured entropy came from the spin of the QD itself, with no external system. Entropy changes resulted from QD transitions between a spinless state with an even number N_0 of electrons to a spinful state with odd N_0+1 electrons. As a result, the N-dependent spin degeneracy of the QD effectively makes up the system whose entropy is being measured, and at a mathematical level it can be analyzed in the same way as the present protocol. The entropic contribution to the QD charge step is thus accounted for in Eq. (1) by $F(N_0) = -T\log 1 = 0$ and $F(N_0+1) = -T\log 2$, yielding a charge step $N(\mu) = N_0 + 2e^{-[E(N_0+1)/T]}/(e^{-[E(N_0)/T]} + 2e^{-[E(N_0+1)/T]})$ that shifts towards smaller μ at higher T. Integrating the area corresponding to this shift [Eq. (2)] gives the expected log2 entropy change as a spinful electron enters the QD [25].

From the point of view of the entropy measurement itself, the case of a Majorana qubit is only slightly more complicated than the simple analysis above, but from a microscopic point of view the thermodynamics of the system in Fig. 1 requires a more careful consideration.

Entropy change of Majorana wire side coupled to a lead.—Consider the total Hamiltonian $H = H_{\rm wire} + H_{\rm wire\text{-}lead} + H_{\rm lead}$. To describe a wire in the topological regime, we consider the Kitaev chain model for $H_{\rm wire}$ [4,31]. The first site of the Kitaev chain, described by fermionic creation operator $a_1^\dagger$, is then coupled via normal hopping $H_{\rm wire\text{-}lead} = t_{\rm WL}a_1^\dagger c_1 + {\rm H.c.}$ to a lead of gapless fermionic excitations, described by a half filled tight-binding chain of length L, $H_{\rm lead} = -t\sum_{j=1}^{L-1}(c_j^\dagger c_{j+1} + {\rm H.c.})$

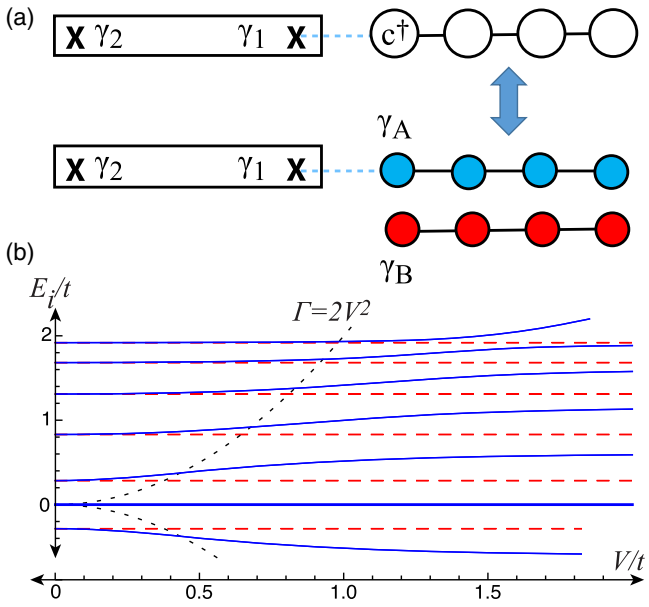

FIG. 2. Absorption of a MZM into a band. (a) Effective model H_{eff} of a Kitaev chain coupled to a lead modeled by a tight-binding chain, and its equivalent in terms of Majoranas in the lead. (b) BdG spectrum for $L = 10$ vs V. All energies are given in units of the tight-binding hopping t.

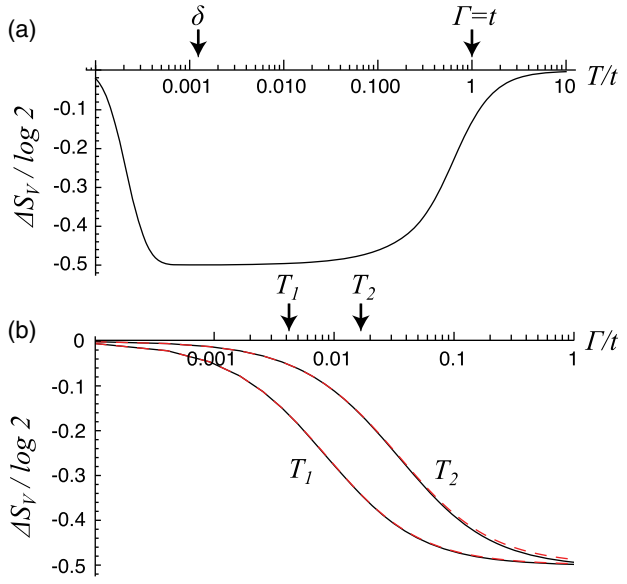

FIG. 3. (a) Entropy vs temperature for the effective model H_{eff} in Fig. 2(a), obtained by numerical diagonalization, illustrating the fractional $-\frac{1}{2}\log 2$ plateau at $\delta \ll T \ll \Gamma$ ($L = 5000$, $t = \Gamma = 1$). (b) Entropy vs wire-lead hybridization Γ at two temperatures T_1, T_2. Γ sets the width of γ_1, and as it decreases below temperature, the universal step $\frac{1}{2}\log 2$ takes place in entropy. Numerical results (solid) are compared with the analytic expression (dashed) obtained using F_{MZM} from the text ($L = 1500$, $T_1 = 0.004t$, $T_2 = 0.016t$).

having level spacing $\delta = (2\pi t/L)$ for large L. In the analysis that follows, we report energy in units of t, a quarter of the bandwidth of the lead and analogous to the Fermi energy in a real system.

Within the topological regime of the wire, that is, at energy scales low compared to the energy gap of H_{wire}, an effective description for the full Hamiltonian H is possible in terms of the pair of MZMs $\gamma_{1,2}$ [Fig. 2(a)], namely, $H_{\text{eff}} = iV(e^{i\phi_1}c_1^\dagger + e^{-i\phi_1}c_1)\gamma_1 + iV_2(e^{i\phi_2}c_1^\dagger + e^{-i\phi_2}c_1)\gamma_2 + i\varepsilon_{12}\gamma_1\gamma_2 + H_{\text{lead}}$. Here, the hopping term between γ_1 and the metallic lead is $V \propto t_{\text{WL}}$ (see Supplemental Material [31]). The phases ϕ_1 and ϕ_2 are set to zero in this Letter, as are the couplings ε_{12}, between the two MZMs, and V_2, between γ_2 and the lead, because both are expected to decay exponentially with the topological wire length. As a result, we have $H_{\text{eff}} \to iV(c_1^\dagger + c_1)\gamma_1 + H_{\text{lead}}$, unless otherwise noted.

It is instructive to first look at the evolution of the single-particle energy levels, i.e., the Bogoliubov–de Gennes (BdG) spectrum of H_{eff}, as the coupling between γ_1 and the lead is turned on [Fig. 2(b)]. For clarity, we consider the case of small L, where the discrete levels are clearly separated. At $V = 0$, the spectrum consists of the levels of the tight-binding chain $E_j = 2t\cos[\pi j/(L+1)]$ $(j = 1, \ldots, L)$ and a doubly degenerate zero energy state from the decoupled MZMs. The effect of V is included by decomposing the tight-binding chain into two Majorana chains denoted A and B in Fig. 2(a). Without loss of generality, the latter can be defined such that γ_1 couples only to the A-Majorana chain (see Supplemental Material [31]).

When V is large, the zero energy level associated with γ_1 is absorbed into the A-Majorana chain, leading to a shift of the other A-Majorana levels [blue in Fig. 2(b)] by approximately half of the level spacing in the lead. The shifting of levels occurs up to an energy scale $\Gamma = 2\,V^2/t$ that depends on V and can be interpreted as the width of γ_1. The B-Majorana chain (red) is unaffected, because it decouples from γ_1 and γ_2 is not coupled to the lead.

The absorption of one MZM into the levels of the lead induces a universal change in the total entropy of the system, for temperatures greater than the level spacing in the lead but less than Γ. This change in entropy is $\Delta S_V \equiv S(V) - S(V = 0)$, where $S(V = 0)$ is the entropy of the isolated tight-binding chain, of order $\mathcal{O}(L)$, plus an extra log2 from the decoupled MZMs.

The drop in entropy induced by coupling to the lead ΔS_V is plotted in Fig. 3 over a wide range of T and Γ. The curve in Fig. 3(a) is obtained from a numerical diagonalization of H_{eff}, followed by a calculation of the entropy $S(V) = -dF/dT$ for the fermionic free energy $F = -T\sum_{E_i}\log(1 + e^{-|E_i|/T})$ [32]. This curve illustrates the characteristic signatures of MZM entropy that underpin the proposed experiment. In the limit of low temperature ($T \ll \delta$), ΔS_V is zero because the system entropy $S = \log 2$

is independent of V: the temperature is not large enough for the chain levels to contribute, leaving only the pair of Majorana states at zero energy. At temperatures larger than the level spacing but less than the width of γ_1, both $S(V)$ and $S(V=0)$ contain $\mathcal{O}(L)$ contributions from the chain levels. The net effect of the coupling then is a reduction by one in the number of Majorana levels within an energy window of T, giving $\Delta S_V = -\frac{1}{2}\log 2$ over the range $\delta \ll T \ll \Gamma$. ΔS_V returns to zero when T rises above Γ. It is this final step in ΔS_V that is detected by the circuit in Fig. 1.

Figure 3(b) compares the numerical diagonalization of $H_{\rm eff}$ to an analytic expression for ΔS_V valid in the continuum limit $\delta \ll T$ and when $\Gamma \ll t$. Its derivation implies a different conceptual framework to understand the $\frac{1}{2}\log 2$ rise of ΔS_V when Γ falls below T. In this approximation, the entropy change is determined by the free energy of the MZMs, $\Delta S_V = -dF_{\rm MZM}/dT - \log 2$, where $F_{\rm MZM} = -T\int_{-\infty}^{\infty} dE\rho(E)\log(1+e^{-|E|/T})$ is determined by the contribution of the MZMs to the density of states in the continuum limit [28,31,33,34], $\rho(E) = \frac{1}{2}\delta(E) + \frac{1}{2}[(\Gamma/\pi)/(\Gamma^2+E^2)]$. The first term in $\rho(E)$ corresponds to the decoupled MZM, γ_2; the second corresponds to the hybridized MZM, γ_1. Both terms contribute $\frac{1}{2}\log 2$ to the entropy for $T \gg \Gamma$, while for $T \ll \Gamma$ only the first term contributes.

Coulomb steps.—The effect of the Γ-induced entropy change on the QD charge steps can be understood using Eq. (1), analogous to the earlier discussion for spinful QDs [25]. For illustration, we analyze the ideal case where a single charge step in the QD results in a transition between limits $\Gamma_0 \gg T$ $(N=0)$ to $\Gamma_1 \ll T$ $(N=1)$. When $N=0$, γ_1 is absorbed in the lead, and the remaining free energy is $F_{\rm MZM}(\Gamma_0) = -(T/2)\ \log 2$ due to γ_2. When $N=1$, $F_{\rm MZM}(\Gamma_1) = -T\log 2$ because both MZMs are free. Using Eq. (1), one finds $N(\mu) = T(d\log Z_{\rm tot}/d\mu) \approx 2e^{-(E_c-\mu)/T}/(\sqrt{2}+2e^{-(E_c-\mu)/T})$ for the $N=0\to 1$ transition, with a charge degeneracy point $N(\mu)=\frac{1}{2}$ that shifts to the left by $-(T/2)\log 2$. In general, degeneracies of consecutive charge states shift by $\Delta\mu_{N,N+1} = F(N+1) - F(N) \simeq -T(S_{N+1} - S_N)$ if the main effect on free energy $F(N)$ is due to entropy S_N.

As a practically relevant example, a sequence of QD charge steps is simulated for a device in which Γ depends exponentially on the barrier height, and therefore on N. Figure 4(a) shows results of this simulation at two temperatures, $T_1 = 0.02$ and $T_2 = 0.04$, where Γ decreases from 1 to 0.0003 across the first two charge steps. The entropy calculated from the integrated difference between $N(\mu)$ at the two temperatures is shown in Fig. 4(b). The entropy rise across the first peak, due to the reduction of Γ from 1 to 0.02, is consistent with the shift of the charge degeneracy point [Fig. 4(a) inset]. The value of this entropy rise is less than the full $\frac{1}{2}\log 2$ because the crossover to $\Gamma \ll T$ is not

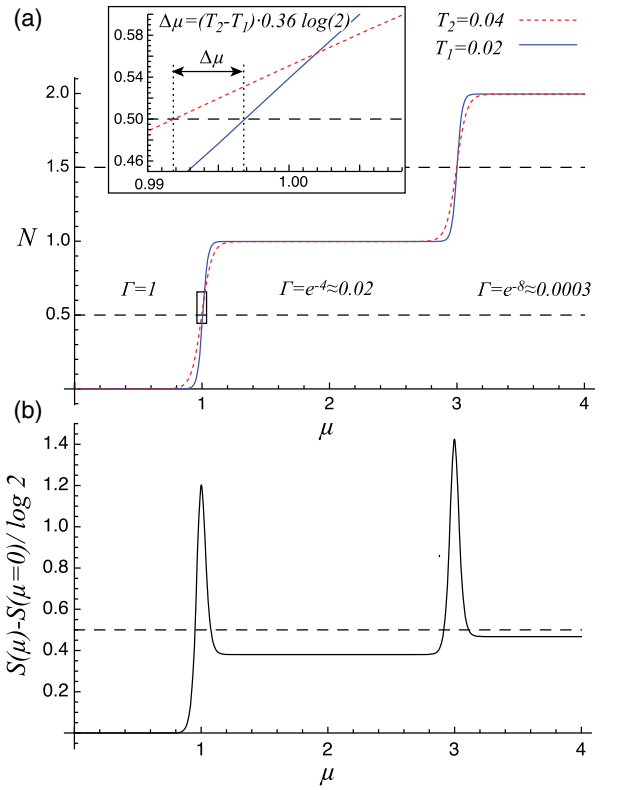

FIG. 4. (a) Coulomb steps of the QD in Fig. 1 for two temperatures $T_1 = 0.02$ and $T_2 = 0.04$ ($E_c = t = 1$). Γ depends exponentially on N as $\Gamma(N) = e^{-4N}$, with calculated values shown in graph. (Inset) Enlargement of the first charge step, showing the shift with temperature $\Delta\mu$ of the charge degeneracy point $N(\mu) = 0.5$. (b) Entropy obtained by integration of $N(\mu)$'s from (a), followed by a discrete T derivative between T_1 and T_2 to approximate Eq. (2).

reached until the next charge step. An additional log2 entropy at $\mu = E_c$ and $3E_c$ is associated with QD charge degeneracy and may be useful for calibration.

Andreev bound states.—The universal entropy signature obtained for MZMs is readily distinguished from that of a regular fermionic level tuned to zero energy. This can be understood from the viewpoint of non topological states (ABSs) as two spatially overlapping MZMs, which would generically couple to the lead with similar magnitudes (see Supplemental Material [31]). Tuning the state to zero energy corresponds to tuning the matrix element between the two MZM wave functions to zero. Depending on the nonuniversal ratio between the two MZM-lead couplings, ΔS_V could range between $\frac{1}{2}\log 2$ and $\log 2$. Only in the case of a simultaneous coincidence [31]—the ABS fine-tuned to zero energy *and* a particular type of asymmetric coupling between the two MZMs to the metallic lead—does the entropic signature fail to identify the non topological character of the ABS. We note that alternative models of emergent low-energy effective Majorana modes, e.g., in dissipative systems [35,36] or the two-channel Kondo

effect [26,27], may give rise to similar entropic signatures as the ones discussed here. Our thermodynamic detection scheme does *not* distinguish between the underlying models, but only indicates the presence or absence of a MZM. In order to determine the usefulness of the MZMs towards topological quantum computing applications in any setting, more challenging braiding or qubit experiments [7] thus remain to be performed.

Experimental observability.—Recent measurements of quantized Majorana conductance [10] imply a Majorana width $\Gamma \sim 50$–$100\ \mu$eV. Since a metallic lead has effectively vanishing level spacing, the requirement $\delta \ll T \ll \Gamma$ for observing the fractionally quantized $\frac{1}{2}\log 2$ entropy change can be readily satisfied. The second key requirement is a sensitive dependence of the wire-lead coupling on the QD charge. To achieve this, one could implement the wire-lead barrier using an unoccupied dot with virtual transport through the first level [37,38].

We thank I. Affleck and A. Mitchell for discussions. This work was partially supported by BSF Grant No. 2016255 (E. S.), by the European Unions Horizon 2020 research and innovation programme (Grant Agreement LEGOTOP No. 788715), the DFG (CRC/Transregio 183, EI 519/7-1519/7-1), and the Israel Science Foundation (ISF) (Y. O.). N. H., S. L., and J. F. were supported by Microsoft, the Canada Foundation for Innovation, the Natural Sciences and Engineering Research Council of Canada, CIFAR, and Stewart Blusson Quantum Matter Institute.

*Corresponding author.
jfolk@physics.ubc.ca
†Present address: Station Q Purdue, Purdue University, West Lafayette, Indiana, USA.

[1] N. Read and D. Green, Phys. Rev. B **61**, 10267 (2000).
[2] L. Fu and C. L. Kane, Phys. Rev. Lett. **100**, 096407 (2008).
[3] J.-P. Xu, M.-X. Wang, Z. L. Liu, J.-F. Ge, X. Yang, C. Liu, Z. A. Xu, D. Guan, C. L. Gao, D. Qian *et al.*, Phys. Rev. Lett. **114**, 017001 (2015).
[4] A. Y. Kitaev, Phys. Usp. **44**, 131 (2001).
[5] Y. Oreg, G. Refael, and F. von Oppen, Phys. Rev. Lett. **105**, 177002 (2010).
[6] R. M. Lutchyn, J. D. Sau, and S. Das Sarma, Phys. Rev. Lett. **105**, 077001 (2010).
[7] R. Lutchyn, E. Bakkers, L. Kouwenhoven, P. Krogstrup, C. Marcus, and Y. Oreg, Nat. Rev. Mater. **3**, 52 (2018).
[8] V. Mourik, K. Zuo, S. M. Frolov, S. Plissard, E. P. Bakkers, and L. P. Kouwenhoven, Science **336**, 1003 (2012).
[9] A. Das, Y. Ronen, Y. Most, Y. Oreg, M. Heiblum, and H. Shtrikman, Nat. Phys. **8**, 887 (2012).
[10] H. Zhang, C.-X. Liu, S. Gazibegovic, D. Xu, J. A. Logan, G. Wang, N. Van Loo, J. D. Bommer, M. W. De Moor, D. Car *et al.*, Nature (London) **556**, 74 (2018).
[11] M. Hell, M. Leijnse, and K. Flensberg, Phys. Rev. Lett. **118**, 107701 (2017).
[12] F. Pientka, A. Keselman, E. Berg, A. Yacoby, A. Stern, and B. I. Halperin, Phys. Rev. X **7**, 021032 (2017).
[13] A. Fornieri, A. M. Whiticar, F. Setiawan, E. Portolés, A. C. Drachmann, A. Keselman, S. Gronin, C. Thomas, T. Wang, R. Kallaher *et al.*, Nature (London) **569**, 89 (2019).
[14] H. Ren, F. Pientka, S. Hart, A. T. Pierce, M. Kosowsky, L. Lunczer, R. Schlereth, B. Scharf, E. M. Hankiewicz, L. W. Molenkamp *et al.*, Nature (London) **569**, 93 (2019).
[15] J. Alicea, Rep. Prog. Phys. **75**, 076501 (2012).
[16] C. Beenakker, Annu. Rev. Condens. Matter Phys. **4**, 113 (2013).
[17] B. A. Schmidt, K. Bennaceur, S. Gaucher, G. Gervais, L. N. Pfeiffer, and K. W. West, Phys. Rev. B **95**, 201306(R) (2017).
[18] K. Yang and B. I. Halperin, Phys. Rev. B **79**, 115317 (2009).
[19] W. E. Chickering, J. P. Eisenstein, L. N. Pfeiffer, and K. W. West, Phys. Rev. B **87**, 075302 (2013).
[20] C.-Y. Hou, K. Shtengel, G. Refael, and P. M. Goldbart, New J. Phys. **14**, 105005 (2012).
[21] Y. Kleeorin, H. Thierschmann, H. Buhmann, A. Georges, L. W. Molenkamp, and Y. Meir, arXiv:1904.08948.
[22] N. R. Cooper and A. Stern, Phys. Rev. Lett. **102**, 176807 (2009).
[23] G. Ben-Shach, C. R. Laumann, I. Neder, A. Yacoby, and B. I. Halperin, Phys. Rev. Lett. **110**, 106805 (2013).
[24] A. Y. Kuntsevich, Y. Tupikov, V. Pudalov, and I. Burmistrov, Nat. Commun. **6**, 7298 (2015).
[25] N. Hartman, C. Olsen, S. Lüscher, M. Samani, S. Fallahi, G. C. Gardner, M. Manfra, and J. Folk, Nat. Phys. **14**, 1083 (2018).
[26] N. Andrei and C. Destri, Phys. Rev. Lett. **52**, 364 (1984).
[27] I. Affleck and A. W. W. Ludwig, Phys. Rev. Lett. **67**, 161 (1991).
[28] V. J. Emery and S. Kivelson, Phys. Rev. B **46**, 10812 (1992).
[29] I. Affleck and D. Giuliano, J. Stat. Mech. (2013) P06011.
[30] S. Smirnov, Phys. Rev. B **92**, 195312 (2015).
[31] See Supplemental Material at http://link.aps.org/supplemental/10.1103/PhysRevLett.123.147702 for an analytic form of the MZM entropy and for a description of ABSs and their entropy.
[32] The sum runs over the non-negative half of the BdG spectrum.
[33] M. Fabrizio, A. O. Gogolin, and P. Nozières, Phys. Rev. B **51**, 16088 (1995).
[34] A. Rozhkov, Int. J. Mod. Phys. B **12**, 3457 (1998).
[35] P. San-Jose, J. Cayao, E. Prada, and R. Aguado, Sci. Rep. **6**, 21427 (2016).
[36] N. Okuma and M. Sato, Phys. Rev. Lett. **123**, 097701 (2019).
[37] M. Deng, S. Vaitiekėnas, E. B. Hansen, J. Danon, M. Leijnse, K. Flensberg, J. Nygård, P. Krogstrup, and C. M. Marcus, Science **354**, 1557 (2016).
[38] M.-T. Deng, S. Vaitiekėnas, E. Prada, P. San-Jose, J. Nygård, P. Krogstrup, R. Aguado, and C. M. Marcus, Phys. Rev. B **98**, 085125 (2018).